

Dual-specificity phosphatase 6 regulates CD4⁺ T-cell functions and restrains spontaneous colitis in IL-10-deficient mice

S Bertin^{1,3}, B Lozano-Ruiz^{2,3}, V Bachiller², I García-Martínez², S Herdman¹, P Zapater², R Francés², J Such², J Lee¹, E Raz¹ and JM González-Navajas^{1,2}

Mitogen-activated protein kinase (MAPK) phosphatases are dual-specificity phosphatases (DUSPs) that dephosphorylate phosphothreonine and phosphotyrosine residues within MAPKs. DUSP6 preferentially dephosphorylates extracellular signal-regulated kinases 1 and 2 (ERK1/2) rendering them inactive. Here, we study the role of DUSP6 in CD4⁺ T-cell function, differentiation, and inflammatory profile in the colon. Upon T-cell receptor (TCR) stimulation, DUSP6 knockout (*Dusp6*^{-/-}) CD4⁺ T cells showed increased ERK1/2 activation, proliferation, T helper 1 differentiation, and interferon- γ production, as well as a marked decrease in survival, interleukin-17A (IL-17A) secretion, and regulatory T-cell function. To analyze the role of DUSP6 *in vivo*, we employed the *Il10*^{-/-} model of colitis and generated *Il10*^{-/-}/*Dusp6*^{-/-} double-knockout mice. *Il10*^{-/-}/*Dusp6*^{-/-} mice suffered from accelerated and exacerbated spontaneous colitis, which was prevented by ERK1/2 inhibition. ERK1/2 inhibition also augmented regulatory T-cell differentiation *in vitro* and *in vivo* in both C57Bl/6 and *Dusp6*^{-/-} mice. In summary, DUSP6 regulates CD4⁺ T-cell activation and differentiation by inhibiting the TCR-dependent ERK1/2 activation. DUSP6 might therefore be a potential intervention target for limiting aberrant T-cell responses in T-cell-mediated diseases, such as inflammatory bowel disease.

INTRODUCTION

Extracellular signal-regulated kinases (ERKs) are central to multiple cellular functions, including growth, differentiation, and survival. ERK1/2 are activated by phosphorylation of Thr and Tyr residues by the upstream kinases MAPK/ERK 1 and 2 (MEK1/2). Once activated, ERK1/2 phosphorylate more than 100 different substrates controlling a variety of biological responses.¹ The activity of ERK1/2 is tightly regulated by feedback mechanisms targeting ERK1/2 itself or its upstream activators. A crucial mechanism of ERK1/2 inactivation is dependent on specific phosphatases with dual specificity for Ser/Thr and Tyr residues and referred to as MAP kinase phosphatases (MKPs), which belong to the dual-specificity phosphatase (DUSP) family.² DUSP6, also called MKP3, is a cytoplasmic member of this family that is highly specific for ERKs.²⁻⁵

DUSP6 expression is constitutive in some cell types, or regulated by several signaling pathways in others. The MEK/ERK pathway can increase *Dusp6* mRNA expression and stability as part of a negative feedback loop.^{6,7} On the other hand, the mammalian target of rapamycin and the MEK/ERK pathways can reduce DUSP6 protein expression by inducing its phosphorylation and subsequent degradation in the proteasome upon stimulation with serum growth factors.^{8,9} Pattern recognition receptor signaling can also regulate DUSP6 expression. Indeed, we have previously shown that DUSP6 is constitutively expressed in CD4⁺ T cells and that TLR4 signaling upregulates its expression, which restrains ERK1/2 activation and interferon- γ (IFN- γ) production upon T-cell receptor (TCR) stimulation.¹⁰

Aberrant T-cell activation is associated with immunological disorders of the gastrointestinal tract, such as inflammatory

¹Division of Rheumatology, Allergy and Immunology, University of California San Diego, La Jolla, California, USA and ²Networked Biomedical Research Center for Hepatic and Digestive Disease (CIBERehd), Institute of Health Carlos III, Madrid, Spain. Correspondence: JM González-Navajas (gonzalez_josnav@gva.es)

³The first two authors contributed equally to this work.

Received 21 January 2014; accepted 7 August 2014; published online 17 September 2014. doi:10.1038/mi.2014.84

bowel disease (IBD). Much of our current understanding of the mechanisms involved in IBD has come from knockout mouse models. Interleukin-10 (IL-10) knockout (*Il10*^{-/-}) mice develop spontaneous chronic enterocolitis with mucosal infiltration of lymphocytes, macrophages, and neutrophils similar to that observed in the mucosal tissues of humans with IBD.¹¹ The enterocolitis in *Il10*^{-/-} mice is largely attributed to dysfunctional CD4⁺ T-cell activation¹² and, as in many other models of intestinal inflammation, the inflammatory response in the intestinal mucosa in this model depends on luminal bacteria or their inflammatory components.^{13,14}

Multiple molecular mechanisms are involved in regulating T-cell development and function. Among others, ERK1/2 activity is crucial for controlling T-cell development,^{15,16} differentiation,^{17,18} and TCR-induced signal strength.¹⁹ However, some controversy exists on the role of ERK pathway in T helper (Th) cell differentiation, particularly in the differentiation of the Th17 lineage.²⁰⁻²² Here, we used homozygous null *Dusp6* (*Dusp6*^{-/-}) mice to study the role of ERK1/2 in T-cell function, differentiation, and pro-inflammatory properties. It was previously shown that *Dusp6*^{-/-} mice have increased basal ERK1/2 phosphorylation in the heart, spleen, kidney, brain, and fibroblasts, but no change in ERK5, p38, or c-Jun activation.⁵ Otherwise these mice are viable, fertile, and grow normally without signs of overt phenotype. We found that DUSP6 deficiency in naive CD4⁺ T cells resulted in increased proliferation and Th1 differentiation *in vitro*. *In vivo*, *Il10*^{-/-}/*Dusp6*^{-/-} mice developed an early-onset of severe colitis, which was ameliorated by ERK1/2 inhibition. Moreover, ERK1/2 inhibition restrained Th1 and Th17 differentiation while enhancing regulatory T-cell (Treg) differentiation. Our data identify DUSP6 as a potential target for limiting aberrant T-cell responses in IBD and other inflammatory disorders.

RESULTS

DUSP6 regulates the TCR-mediated activation, proliferation, and survival of CD4⁺ T cells

Although the expression of DUSP6 in naive CD4⁺ T cells has been reported in mice and humans,^{10,23,24} the role of DUSP6 in CD4⁺ T-cell activation and function has not been examined. We observed a time-dependent increase in DUSP6 protein expression after TCR or TLR4 stimulation of splenic CD4⁺ T cells from wild-type (WT) mice with anti-CD3/28 antibodies or lipopolysaccharide, respectively (**Figure 1a**). Next, we isolated CD4⁺ T cells from WT and *Dusp6*^{-/-} mice to investigate the role of this phosphatase in CD4⁺ T-cell functions. TCR stimulation of *Dusp6*^{-/-} CD4⁺ T cells resulted in higher phosphorylation levels of ERK1/2, but not of p38 or JNK1/2 MAPKs compared with WT cells (**Figure 1b**). We then analyzed the cytokine production by CD4⁺ T cells collected from the spleen and mesenteric lymph nodes (MLNs) of WT and *Dusp6*^{-/-} mice and stimulated with anti-CD3/28 antibodies. Although there was no significant difference in the production of IL-2, 4, 6, and 10, we found that *Dusp6*^{-/-} CD4⁺ T cells, from both MLNs (**Figure 1c**) and spleen (**Supplementary Figure S1** online), produced higher amounts

of IFN- γ and lower amounts of IL-17A when compared with WT CD4⁺ T cells. In accordance with the cytokine data, TCR stimulation of splenic *Dusp6*^{-/-} CD4⁺ T cells resulted in a transcriptional increase in the Th1-related transcription factor T-box expressed in T cells, as well as in a decrease in the Th17-related RAR-related orphan receptor γ t, whereas the expression of GATA-binding protein 3 and forkhead box P3 (FOXP3), which function as master regulators of Th2 and Treg cells, respectively, remained unaltered when compared with WT CD4⁺ T cells (**Figure 1d**).

To further delineate the role of DUSP6 in CD4⁺ T cells, we compared the development, proliferation, and survival of CD4⁺ T cells isolated from WT and *Dusp6*^{-/-} mice. The percentages of CD4⁺, CD8⁺, and CD4/CD8 double-positive cells in the spleen, MLN, and thymus of *Dusp6*^{-/-} mice were not significantly different from WT mice (**Supplementary Figure S2a**), neither was different the amount of total cells in these organs (**Supplementary Figure S2b**). However, despite having comparable numbers of total CD4⁺ T cells, the amount of memory-effector CD4⁺ T cells (CD44^{high}) was augmented, while the number of naive CD4⁺ T cells (CD44^{low}CD62L^{high}) was reduced in the spleens of *Dusp6*^{-/-} mice (**Figure 2a**), indicative of an increased CD4⁺ T-cell activation in these mice. Furthermore, in cellular proliferation assays with 5,6-carboxyfluorescein diacetate succinimidyl ester (CFSE) staining, *Dusp6*^{-/-} CD4⁺ T cells displayed increased proliferation upon stimulation with anti-CD3/28 antibodies (**Figure 2b**), which is consistent with previous reports in human CD4⁺ T cells.²³ The increased proliferation capacity of *Dusp6*^{-/-} CD4⁺ T cells was confirmed by bromodeoxyuridine incorporation assay (**Supplementary Figure S3a** and **b**). Unexpectedly, *Dusp6*^{-/-} CD4⁺ T cells also showed increased activation-induced cell death as evidenced by the lower percentage of viable cells observed by Trypan blue exclusion method (**Figure 2c**), as well as by the increase in late-stage apoptotic cells (Annexin V⁺ and 7-AAD⁺) and total Annexin V⁺ cells detected by flow cytometry analysis after TCR stimulation (**Figure 2d** and **e**). Consistent with these data, the mRNA levels of the pro-apoptotic markers FasL and Caspase-3 were also elevated in *Dusp6*^{-/-} CD4⁺ T cells upon stimulation with anti-CD3/28 antibodies (**Figure 2f**). These data might explain why *Dusp6*^{-/-} mice show equal numbers of CD4⁺ T cells in lymphoid organs (**Supplementary Figure S2**) despite having superior proliferative responses (**Figure 2b**). Taken together, these data indicate that the lack of DUSP6 expression affects TCR-dependent responses in CD4⁺ T cells, including cytokine production, proliferation, and survival.

Because *Dusp6* mRNA expression in CD8⁺ T cells was comparable with CD4⁺ T cells (**Supplementary Figure S4a**), we next sought to investigate whether DUSP6 also modulates the responses of CD8⁺ T cells. Whereas IFN- γ production in CD8⁺ T cells from *Dusp6*^{-/-} mice was normal (**Supplementary Figure S4b**), surface expression of CD107a (also known as lysosomal-associated membrane protein 1, LAMP-1), which occurs during T-cell degranulation following antigenic stimulation,^{25,26} was reduced in *Dusp6*^{-/-} CD8⁺ T cells

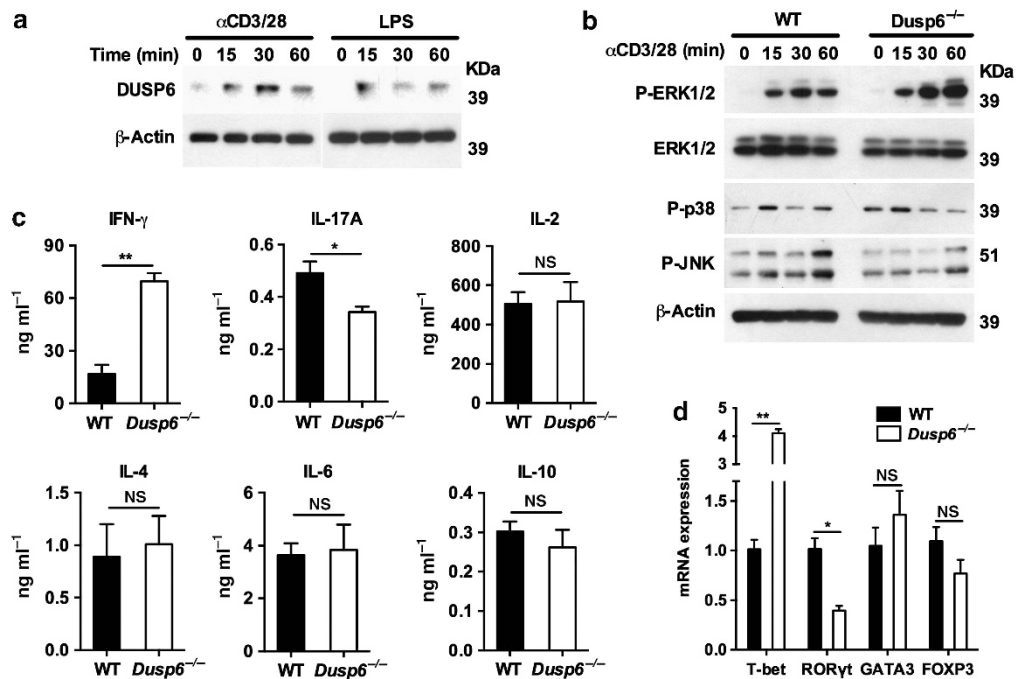


Figure 1 Increased ERK1/2 activation and IFN- γ production in *Dusp6*^{-/-} CD4⁺ T cells. (a) Immunoblot analysis of DUSP6 expression in CD4⁺ T cells from WT mice upon activation of either TLR4 (100 μ g LPS) or T-cell receptor (α CD3/28 antibodies). (b) Immunoblot analysis of phosphorylated levels of MAPKs in CD4⁺ T cells stimulated with anti-CD3/28 antibodies for the indicated time points. Data are representative of three independent experiments (a, b). (c) Cytokine levels in culture supernatants of mesenteric lymph node-derived CD4⁺ T cells isolated from WT and *Dusp6*^{-/-} mice and stimulated with anti-CD3/28 antibodies for 24 h ($n \geq 9$ mice per group). (d) Quantitative PCR analysis of the expression of different transcription factors in CD4⁺ T cells from WT and *Dusp6*^{-/-} mice stimulated with anti-CD3/28 antibodies ($n \geq 5$ mice per group). The mRNA fold induction in *Dusp6*^{-/-} CD4⁺ T cells was normalized according to the mRNA expression in WT T cells. Glyceraldehyde-3-phosphate dehydrogenase was used as internal control. Error bars represent standard deviation. Data represent results from either three (a–c) or two (d) independent experiments. * $P < 0.05$, ** $P < 0.01$. DUSP, dual-specificity phosphatase; IFN, interferon; IL, interleukin; LPS, lipopolysaccharide; NS, nonsignificant; WT, wild type.

(Supplementary Figure S4c). These results suggest that DUSP6 may also play a role in the cytotoxic activity of CD8⁺ T cells.

Th1 differentiation is enhanced in DUSP6-deficient CD4⁺ T cells

Our previous observations showing a different production of IFN- γ and IL-17A by *Dusp6*^{-/-} CD4⁺ T cells (Figure 1 and Supplementary Figure S1) suggested that DUSP6 might be involved in the differentiation of Th cell subsets. To test this hypothesis, we isolated naive CD4⁺ T cells from the spleen of WT and *Dusp6*^{-/-} mice by fluorescence-activated cell sorter (FACS) sorting, and cultured them under Th1 or Th17 polarizing conditions. After 5 days of differentiation *in vitro*, we re-stimulated the cells with anti-CD3/CD28 antibodies and analyzed IFN- γ and IL-17A production by FACS intracellular staining and ELISA. Under Th1 conditions, the number of IFN- γ -producing cells was increased in *Dusp6*^{-/-} CD4⁺ T cells when compared with WT T cells (Figure 3a). Consistent with these data, the protein level of IFN- γ was also increased in culture supernatants of *Dusp6*^{-/-} CD4⁺ T cells (Figure 3b). By contrast, under Th17 polarizing conditions, we found that both the number of IL-17A-producing cells and the level of IL-17A in culture supernatants were diminished in *Dusp6*^{-/-} CD4⁺ T cells when compared with WT control cells (Figure 3c and d). These data suggest that DUSP6 regulates the develop-

ment of CD4⁺ T-cell subsets by inhibiting Th1 differentiation and favoring Th17 differentiation.

DUSP6 deficiency reduces the suppressive ability of regulatory CD4⁺ T cells

Recent reports have shown that ERK1/2 suppresses the differentiation of FOXP3⁺ Treg cells and that its inhibition enhances Treg cell development while limiting Th1 and Th17 development.^{17,18,21} To determine the impact of DUSP6 in Treg cell differentiation, we analyzed the amount of FOXP3⁺ CD4⁺ T cells in *Dusp6*^{-/-} mice *in vivo* and the ability of *Dusp6*^{-/-} naive CD4⁺ T cells to differentiate into Tregs *in vitro*. As shown in Figure 4a, the percentages of FOXP3⁺ CD4⁺ T cells in the spleen and MLN of *Dusp6*^{-/-} mice were similar to those of WT mice. In addition, *Dusp6*^{-/-} naive CD4⁺ T cells showed normal capacity to differentiate into FOXP3⁺ Treg cells *in vitro* (Supplementary Figure S5). In agreement with the current literature,^{17,18,21} treatment with PD0325901 (PD), a selective pharmacological inhibitor of ERK,^{27,28} resulted in increased Treg cell polarization of both WT and *Dusp6*^{-/-} naive CD4⁺ T cells (Supplementary Figure S5). To determine whether ERK inhibition could also induce Treg cell differentiation *in vivo*, we administered PD orally to WT and *Dusp6*^{-/-} mice once a day for a total period of 10 days, and then analyzed the expression of FOXP3 in freshly isolated

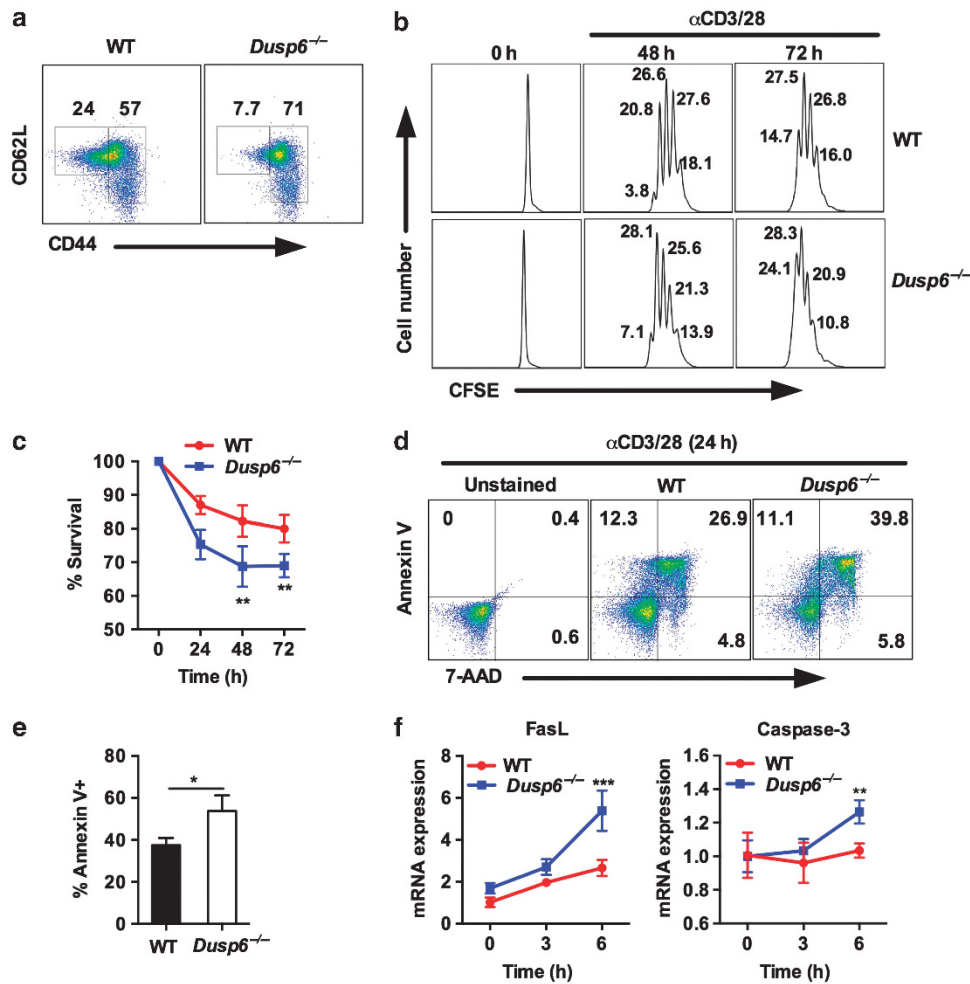


Figure 2 DUSP6 deficiency results in increased proliferation and activation-induced cell death. (a) Flow cytometry analysis of the naive (CD44^{low}CD62L^{high}) and activated (CD44^{high}) CD4⁺ T-cell populations in the spleens of WT and *Dusp6*^{-/-} mice. (b) Proliferation assay by flow cytometry analysis of the fluorescence intensity of CFSE-labeled naive T cells from WT and *Dusp6*^{-/-} mice after 48 and 72 h of T-cell receptor stimulation with anti-CD3/28 antibodies. Data are representative of two independent experiments (a, b). (c) Percent of viable CD4⁺ T cells measured by microscopic evaluation using the Trypan blue exclusion method in WT and *Dusp6*^{-/-} T cells stimulated with anti-CD3/CD28 antibodies. Data represent pooled results from three independent experiments; ***P* < 0.01. (d) Flow cytometry analysis of early apoptotic (Annexin V⁺, 7-AAD⁻), late-stage apoptotic (Annexin V⁺, 7-AAD⁺), and necrotic (Annexin V⁻, 7-AAD⁺) CD4⁺ T cells after 24 h of stimulation with anti-CD3/28 antibodies. Data are representative of three independent experiments (*n* = 3 mice per group). (e) Statistical analysis of the percentage of total Annexin V⁺ cells is shown in d. Data represent pooled results from three independent experiments (*n* = 3 mice per group). (f) Quantitative PCR analysis of pro-apoptotic genes in WT and *Dusp6*^{-/-} CD4⁺ T cells stimulated with anti-CD3/28 antibodies. Data represent pooled results from two experiments (*n* = 3 mice per group). Error bars represent s.d. ***P* < 0.01, ****P* < 0.001. CFSE, 5,6-carboxyfluorescein diacetate succinimidyl ester; DUSP, dual-specificity phosphatase; WT, wild type.

splenic CD4⁺ T cells. Indeed, PD treatment augmented the number of FOXP3⁺CD4⁺ T cells in both WT and *Dusp6*^{-/-} mice (Figure 4b). Next, we sought to determine whether the lack of DUSP6 expression affects the suppressive capacity of Tregs. To do so, we isolated naive CD4⁺ T cells from WT mice, labeled them with CFSE, and co-cultured them with unlabeled WT or *Dusp6*^{-/-} Treg cells (CD4⁺CD45RB^{low}CD25⁺) at a ratio of 1:4 (Treg:Tnaive), and stimulated them for 72 h in the absence of antigen-presenting cells as previously described.²⁹ Interestingly, when compared with WT Tregs, DUSP6-deficient Treg cells showed reduced ability to suppress the proliferation of naive CD4⁺ T cells (Figure 4c and d). We obtained similar results at 1:8 and 1:16 Treg:Tnaive ratios (Supplementary Figure S6). Taken together, our data suggest

that DUSP6 deficiency affects the suppressive ability of FOXP3⁺ regulatory CD4⁺ T cells.

DUSP6 deficiency aggravates IL-10-dependent colitis

We have previously shown that TLR4 regulates the inflammatory profile of CD4⁺ T cells and exerts a tonic inhibition on certain TCR signaling events via the induction of DUSP6.¹⁰ Furthermore, the data shown herein suggest that DUSP6 exerts important regulatory functions in CD4⁺ T cells that may affect their pro- and anti-inflammatory potential. To delineate the role of this phosphatase in the development of colitis, we crossed *Dusp6*^{-/-} mice onto *Il10*^{-/-} animals to generate *Il10*^{-/-}/*Dusp6*^{-/-} double-knockout mice. We then co-housed 4-week-old *Il10*^{-/-} and *Il10*^{-/-}/*Dusp6*^{-/-} mice

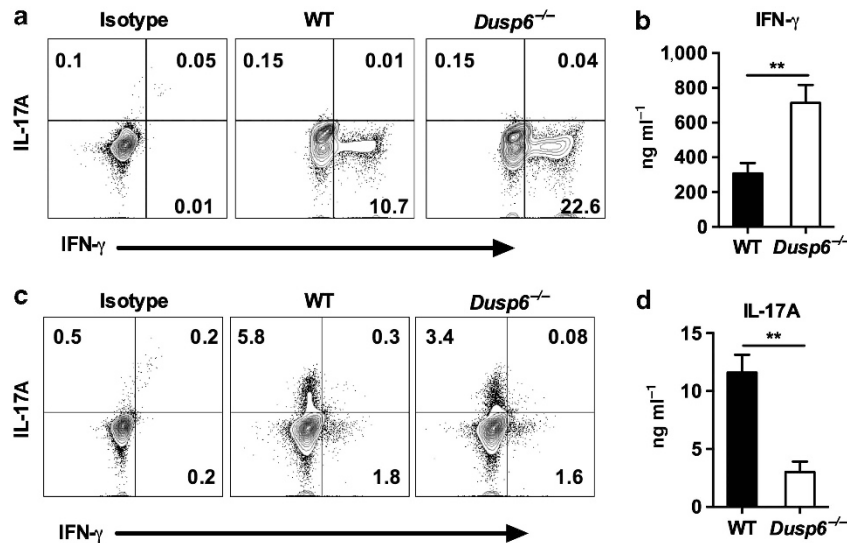


Figure 3 DUSP6 deficiency facilitates Th1 differentiation *in vitro*. (a and c) Flow cytometry analysis of intracellular cytokines in naive CD4⁺ T cells from WT and *Dusp6*^{-/-} mice cultured in Th1 (a) or Th17 (c) polarizing conditions for 5 days, and re-stimulated with anti-CD3/28 antibodies for 6 h. (b and d) Cytokine levels measured by ELISA in supernatants of naive T cells cultured in Th1 (b) or Th17 (d) conditions and re-stimulated with anti-CD3/28 antibodies for 48 h. Data in this figure represent pooled results from four independent experiments. Error bars represent s.d. ***P* < 0.01. DUSP, dual-specificity phosphatase; IFN, interferon; IL, interleukin; WT, wild type.

to allow colonization of these two groups with the same microflora,³⁰ and followed them weekly for signs of inflammation for an additional period of 6 months. Although *Il10*^{-/-} mice did not show intestinal inflammation at the age of 7 months, *Il10*^{-/-}/*Dusp6*^{-/-} mice displayed macroscopic signs of intestinal inflammation between 10 and 14 weeks of age, such as diarrhea and thickening of the intestinal wall (Supplementary Figure S7). Histological evaluation (Figure 5a) and quantitative morphometric analysis (Figure 5b) of the colon revealed that *Il10*^{-/-}/*Dusp6*^{-/-} mice developed severe inflammation with a high degree of epithelial crypt hyperplasia, goblet-cell depletion, and infiltration of mononuclear cells in the colonic lamina propria. To quantify the inflammatory mediators produced by the inflamed colons, we cultured *ex vivo* colonic explants from *Il10*^{-/-} and *Il10*^{-/-}/*Dusp6*^{-/-} mice. Colonic explants from *Il10*^{-/-}/*Dusp6*^{-/-} mice released high amounts of IFN-γ and tumor necrosis factor-α, whereas the level of IL-17A was lower than in the supernatants harvested from *Il10*^{-/-} colonic explants (Figure 5c). To further evaluate the inflammatory phenotype of these mice, effector CD4⁺ T cells were isolated from MLNs and spleen, and stimulated with anti-CD3/28 antibodies. Similar to *Dusp6*^{-/-} mice, MLN-derived CD4⁺ T cells from *Il10*^{-/-}/*Dusp6*^{-/-} mice produced higher levels of IFN-γ but lower levels of IL-17A when compared with CD4⁺ T cells from *Il10*^{-/-} mice (Figure 5d). Similar results were obtained with splenic CD4⁺ T cells (Supplementary Figure S8). In line with the increased ERK1/2 phosphorylation observed in *Dusp6*^{-/-} CD4⁺ T cells (Figure 1b), we found that *Il10*^{-/-}/*Dusp6*^{-/-} CD4⁺ T cells also show elevated phosphorylation levels of ERK1/2 upon stimulation with anti-CD3/28 antibodies (Figure 5e) while the phosphorylation of

p38 or JNK remained unaffected (data not shown). Taken together, these data demonstrate that the lack of DUSP6 expression accelerates intestinal inflammation in genetically susceptible hosts (i.e., *Il10*^{-/-} mice), and impacts the inflammatory cytokine profile of IL-10-deficient CD4⁺ T cells.

ERK inhibition ameliorates colitis in *Il10*^{-/-}/*Dusp6*^{-/-} mice

Our data showing that CD4⁺ T cells from *Dusp6*^{-/-} and *Il10*^{-/-}/*Dusp6*^{-/-} mice had increased levels of phosphorylated ERK1/2 as well as superior IFN-γ production, together with previous data showing that ERK1/2 promotes colitis by inducing an exacerbated IFN-γ response,¹⁰ suggested a potential ERK1/2-dependent mechanism driving the pathogenesis of colitis in *Il10*^{-/-}/*Dusp6*^{-/-} mice. As colitis in *Il10*^{-/-}/*Dusp6*^{-/-} mice was detected by 10 weeks of age, we administered the ERK inhibitor to 5-week-old *Il10*^{-/-}/*Dusp6*^{-/-} mice five times a week for a period of 10 weeks. Vehicle-treated mice developed severe colonic inflammation by the age of 15 weeks, whereas PD treatment significantly reduced the severity of colitis as shown by the lower degree of epithelial crypt hyperplasia and inflammatory cell infiltration into the lamina propria (Figure 6a and b). In addition, *ex vivo* colonic explants from PD-treated *Il10*^{-/-}/*Dusp6*^{-/-} mice also released lower amounts of IFN-γ and tumor necrosis factor-α than vehicle-treated mice (Figure 6c).

Next we aimed to determine whether PD treatment was also able to ameliorate the severity of colitis after it was already established in *Il10*^{-/-}/*Dusp6*^{-/-} mice. Six months old *Il10*^{-/-}/*Dusp6*^{-/-} mice with macroscopic signs of intestinal inflammation were treated with the ERK inhibitor three times a week for a period of 6 weeks. Interestingly, PD

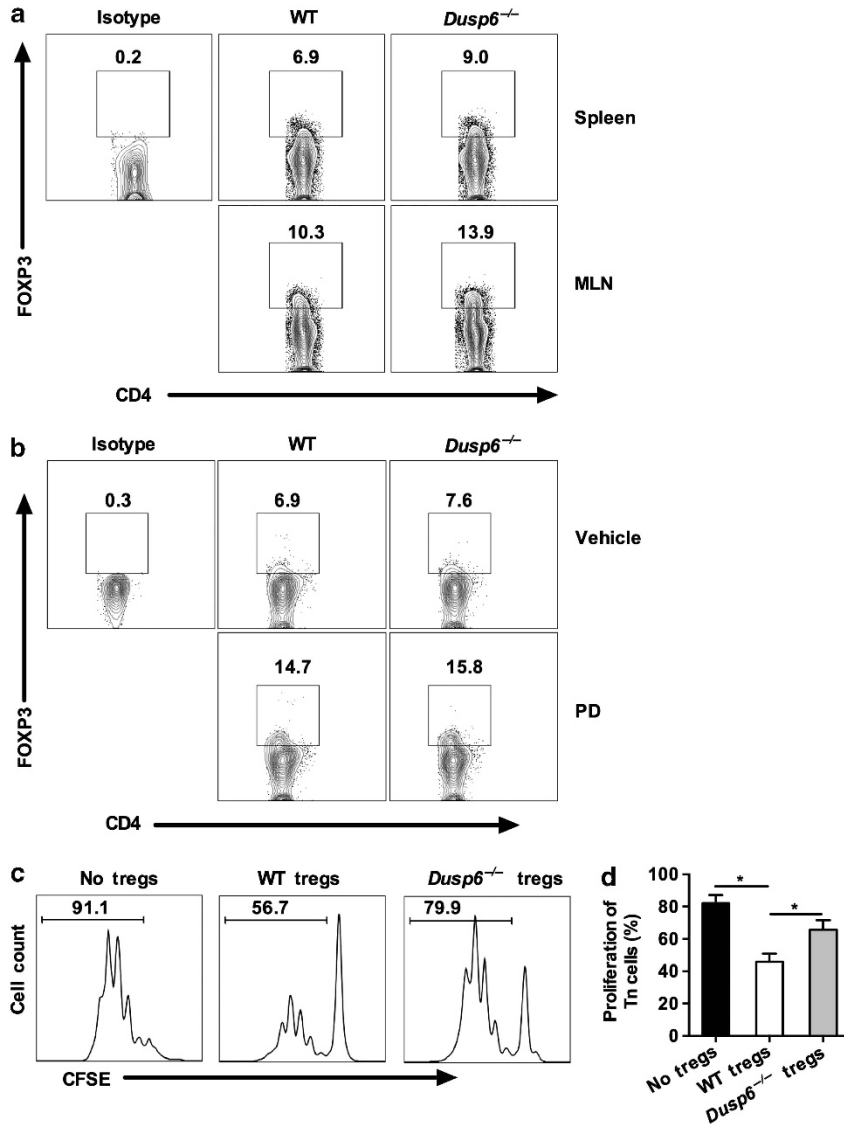


Figure 4 DUSP6 deficiency reduces the suppressive ability of regulatory T cells (Tregs). (a) Flow cytometry analysis of FOXP3 expression in freshly isolated CD4⁺ T cells from the spleen and mesenteric lymph node of WT and *Dusp6*^{-/-} mice. Numbers within the graphs denote the percentage of FOXP3⁺ cells when compared with cells stained with isotype antibody. (b) Flow cytometry analysis of FOXP3 expression in splenic T cells from WT and *Dusp6*^{-/-} mice after oral administration of ERK1/2 inhibitor PD0325901 (PD) or vehicle solution for 10 days. (c) Proliferation analysis of CFSE-labeled naive T cells from WT mice stimulated with anti-CD3/28 antibodies for 72 h and co-cultured with Tregs (CD4⁺CD45RB^{low}CD25⁺) isolated from the spleens of WT or *Dusp6*^{-/-} mice. Cells were co-cultured at a ratio of 1:4 (Treg:Tnaive). (d) Percentage of proliferating naive CD4⁺ T cells from WT mice co-cultured with either WT or *Dusp6*^{-/-} Tregs at a ratio of 1:4 (Treg:Tnaive). Data are representative of either 3 (a, b) or 2 (c, d) independent experiments (n=3 mice per group). CSFE, 5,6-carboxyfluorescein diacetate succinimidyl ester; DUSP, dual-specificity phosphatase; WT, wild type.

treatment resulted in a significant increase in body weight, whereas vehicle-treated mice continued losing weight during the course of the experiment (Supplementary Figure S9a). PD-treated mice also showed a significant amelioration in histologic inflammation, including the recovery of goblet cells and the reduction of epithelial crypt hyperplasia and inflammatory cell infiltration into the lamina propria (Supplementary Figure S9b and c). Furthermore, MLN-derived CD4⁺ T cells isolated from PD-treated mice secreted lower amounts of inflammatory cytokines after stimulation with anti-CD3/28 antibodies (Supplementary Figure S9d). Collectively, these data suggest that the severity of colitis

in *Il10*^{-/-}/*Dusp6*^{-/-} mice is mediated by the increase in ERK1/2 activation.

DISCUSSION

Although there has been particular focus on the role of DUSPs in different aspects of immune regulation and cancer,³¹⁻³³ the role of DUSP6 in inflammatory diseases has not been defined. Here, we analyzed the impact of DUSP6 deficiency in the differentiation and function of CD4⁺ T cells and we utilized the IL-10-dependent model of spontaneous colitis to delineate the role of DUSP6 during chronic inflammation. We found that DUSP6-deficient CD4⁺ T cells have increased ERK1/2

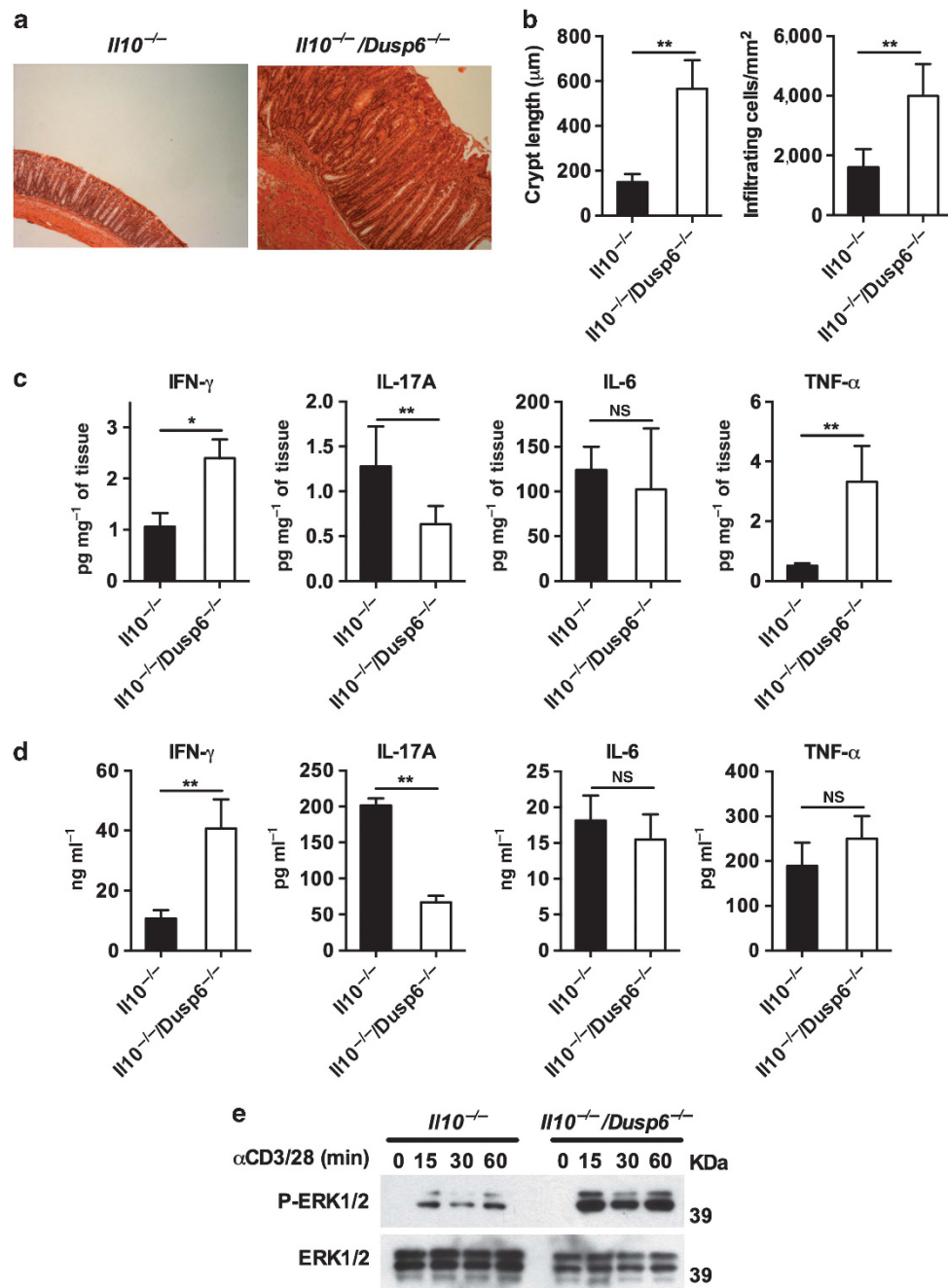


Figure 5 DUSP6 deficiency aggravates colitis in the IL-10 model. (a) Paraffin-embedded colon samples were sectioned and stained with hematoxylin and eosin. Representative micrograph (magnification $\times 100$) of co-housed 12-week-old *Il10^{-/-}* and *Il10^{-/-}/Dusp6^{-/-}* mice maintained under specific pathogen-free conditions ($n \geq 10$ mice per group). (b) Quantitative measurement of crypt length and cellular infiltration in the different groups of mice at 12 weeks of age ($n \geq 10$ mice per group). (c) Cytokine levels in colonic explant supernatants after 24 h of culture. Represented values are normalized to milligrams of cultured colonic tissue. (d) Cytokine levels in culture supernatants of mesenteric lymph node-derived CD4^+ T cells isolated from *Il10^{-/-}* and *Il10^{-/-}/Dusp6^{-/-}* mice and stimulated with anti-CD3/28 antibodies for 24 h. Data represent pooled results from two independent experiments with at least six mice per group (c, d). (e) Immunoblot analysis of phosphorylated levels of ERK1/2 in splenic CD4^+ T cells from both groups of mice stimulated with anti-CD3/28 antibodies for the indicated time points. Data are representative of three independent experiments. Error bars represent s.d., * $P < 0.05$, ** $P < 0.01$. DUSP, dual-specificity phosphatase; IFN, interferon; IL, interleukin; NS, nonsignificant; TNF, tumor necrosis factor; WT, wild type.

activation and production of IFN- γ upon TCR stimulation (Figure 1 and Supplementary Figure 1). *Dusp6^{-/-}* naive CD4^+ T cells also exhibited a greater propensity to differentiate along the Th1 axis *in vitro* (Figure 3). Therefore, it is plausible

that DUSP6 is involved in T-cell-dependent inflammatory disorders. Indeed, we could detect severe spontaneous colitis in 10-week-old *Il10^{-/-}/Dusp6^{-/-}* mice, whereas signs of colitis were undetectable in 7-month-old *Il10^{-/-}* mice (Figure 5).

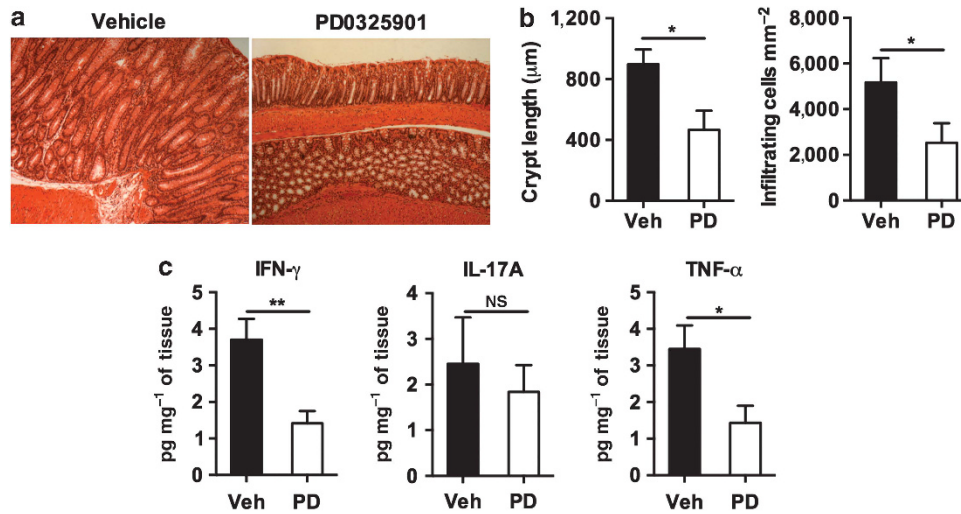


Figure 6 ERK inhibition ameliorates colitis in *Il10*^{-/-}/*Dusp6*^{-/-} mice. (a) Hematoxylin and eosin staining of *Il10*^{-/-}/*Dusp6*^{-/-} mice treated with the MEK1/2 inhibitor PD0325901 (PD) or vehicle five times a week for a total of 10 weeks. Representative micrographs are shown (magnification $\times 100$; $n = 6$ mice per group). (b) Quantitative measurement of crypt length and cellular infiltration in vehicle-treated or PD-treated mice. (c) Cytokine levels in colonic explant supernatants after 24 h of culture. Represented values are normalized to milligrams of cultured colonic tissue. Data represent pooled results from two independent experiments with at least four mice per group (b, c). Error bars represent s.d. * $P < 0.05$, ** $P < 0.01$. DUSP, dual-specificity phosphatase; IFN, interferon; IL, interleukin; NS, nonsignificant; TNF, tumor necrosis factor; WT, wild type.

Moreover, ERK1/2 and IFN- γ protein levels were elevated in colons of *Il10*^{-/-}/*Dusp6*^{-/-} mice, whereas IL-17A was reduced.

The colitis observed in IL-10-deficient mice mainly depends on CD4⁺ T cells¹² and was originally described as a Th1-mediated inflammation, which could be ameliorated by neutralizing antibodies against IL-12p40 or IFN- γ .^{11,34} Later, Th17 cells were shown to participate in the colonic immunopathology in these mice.³⁵ Although it is likely that these two inflammatory cytokines contribute to the development of colitis at different stages,³⁶ the colitis in *Il10*^{-/-}/*Dusp6*^{-/-} mice appears to be exacerbated by IFN- γ , but not IL-17A. Our data also indicate that DUSP6 deficiency reduces the ability of Treg cells to suppress the proliferation of naive CD4⁺ T cells *in vitro*, independently of the expression of FOXP3 (Figure 4). Thus, DUSP6 enhances the regulatory function of Treg cells and inhibits the inflammatory function of activated effector CD4⁺ T cells. In addition, data collected in our laboratory showed that depletion of the CD4⁺ population by administration of anti-CD4 antibodies into *Il10*^{-/-}/*Dusp6*^{-/-} mice resulted in significant inhibition of intestinal inflammation (data not shown). While these data, together with the data shown herein, suggest that CD4⁺ T cells have a key role in the colitis of *Il10*^{-/-}/*Dusp6*^{-/-} mice, we cannot exclude the possibility that other cells than CD4⁺ T cells can also contribute to the severity of the colitis in these mice. The definitive confirmation would require the use of *Il10*^{-/-} mice with targeted deletion of DUSP6 in CD4⁺ T cells.

Controversial data have been reported on the role of ERK signaling in Th17 differentiation. Liu *et al.*²¹ reported that blockade of ERK1/2 activation inhibited Th17 cell development while upregulating Treg cells. By contrast, another study showed that inhibition of ERK signaling enhanced Th17 cell

differentiation and increased the ability of Th17 cells to induce autoimmunity *in vivo*.²² Furthermore, ERK activation was shown to inhibit Th17 cell differentiation through the down-regulation of signal transducer and activator of transcription -3 phosphorylation.²⁰ In agreement with this, our data indicated that DUSP6 deficiency in CD4⁺ T cells reduces Th17 differentiation (Figure 3). The discrepancy between our data and the study by Liu *et al.*²¹ may be explained by the different experimental conditions involved in the use of different ERK pharmacological inhibitors, such as UO126 or PD98059, compared with the use of CD4⁺ T cells with a genetic predisposition to increased ERK1/2 activation (i.e., DUSP6 deficiency).

Apart from ERK1/2, DUSP6 can also dephosphorylate ERK5, another MAP kinase family member downstream of MEK5 that is activated by different stimuli.^{8,37} Therefore it was conceivable that the enterocolitis observed in the absence of DUSP6 was in part because of ERK5 activation. However, the colitis in *Il10*^{-/-}/*Dusp6*^{-/-} mice was completely abolished after treatment with a highly specific MEK1/2 inhibitor (Figure 6 and Supplementary Figure S9), which indicates that the ERK1/2 pathway is responsible for the phenotype in these mice. DUSPs are tightly regulated under inflammatory conditions. Glucocorticoids or IL-10 can induce DUSP1 expression,^{38,39} whereas IFN- γ attenuates it and therefore enhances MAPK activation.⁴⁰ In addition, we have previously shown that activation of MKPs, such as DUSP1 and DUSP6, in CD4⁺ T cells by TLR4 signaling restrains subsequent TCR-induced phosphorylation of MAPKs and therefore modulates CD4⁺ T-cell inflammatory responses.¹⁰ Our findings shown herein expand this knowledge to include the effects of DUSP6 on CD4⁺ T-cell differentiation, survival, proliferation, and regulatory function.

Our data support a role for DUSP6 in the IL-10-deficient model of colitis, yet further investigations will be necessary to better define the role of DUSP6 in innate immune responses and to elucidate if DUSP6 is involved in other models of inflammation-associated diseases.

Finally, our results identify DUSP6 as a potential intervention target for restoring T-cell homeostasis. In particular, increasing DUSP6 expression or function may be a novel strategy for dampening the TCR-induced activation of ERK and IFN- γ in IBD and potentially in other Th1-mediated diseases.

METHODS

Mice. Seven- to twelve-week-old mice were used for all the experimental procedures. C57Bl/6 (i.e., WT) and *Il10*^{-/-} mice on the C57Bl/6 background were originally purchased from The Jackson Laboratory (Bar Harbor, ME) and maintained under specific pathogen-free conditions in our vivarium. *Dusp6*^{-/-} mice on the B6 background were kindly provided by Dr J Molkentin (Cincinnati Children's Hospital Medical Center, Cincinnati, OH) and have been described before.⁵ To generate the double-knockout mice, *Il10*^{-/-} mice were intercrossed with *Dusp6*^{-/-} mice. For colitis studies, *Il10*^{-/-} and *Il10*^{-/-}/*Dusp6*^{-/-} mice were co-housed. The Institutional Animal Care and Use Committee of the UCSD approved all experimental procedures.

Antibodies and reagents. Monoclonal anti-mouse CD3 ϵ (145-2c11) and anti-mouse CD28 (PV-1) antibodies were purchased from BioXcell (West Lebanon, NH). For immunoblot assays the following antibodies were used: anti-DUSP6 (EPR129Y) was purchased from Abcam (Cambridge, MA); anti-phospho-ERK1/2 (D13.14.4E), anti-phospho-p38 (D3F9), anti-phospho-JNK (81E11), and anti-ERK1/2 (137F5) were purchased from Cell Signaling Technologies (Danvers, MA); anti- β -actin (AC-15) was purchased from Sigma-Aldrich (St Louis, MO). For FACS analysis the anti-mouse antibodies anti-CD44 (IM7), anti-CD62L (MEL-14), anti-CD4⁺ (GK1.5), anti-CD8 (53-6.7), anti-Foxp3 (FJK-16s), anti-IFN- γ (XMG1.2), and anti-IL-17A (eBio17B7) were purchased from eBioscience (La Jolla, CA). Annexin V-PE Apoptosis Detection Kit I was purchased from BD Biosciences (San Jose, CA). The MEK inhibitor PD0325901 was purchased from Sigma-Aldrich.

Culture, stimulation, and differentiation of CD4⁺ T cells. Complete RPMI 1640 or IMDM medium (Life Technologies, Carlsbad, CA) supplemented with 10% heat-inactivated fetal calf serum, 2 mM L-glutamine, 100 U ml⁻¹ penicillin, and 100 μ g ml⁻¹ streptomycin was used throughout the experiments. CD4⁺ T cells were isolated from a single-cell suspension of splenocytes or MLN cells by immunomagnetic selection using a EasySep CD4⁺ negative selection Kit (StemCell Technologies, Vancouver, BC, Canada). Purity of the enriched population was >95% in all experiments. After enrichment, cells were cultured in complete RPMI medium and stimulated with 5 μ g ml⁻¹ plate-bound anti-CD3 and 1 μ g ml⁻¹ soluble anti-CD28 antibodies throughout the experiments. Twenty-four and forty-eight hours culture supernatants were collected for cytokine analysis using Ready-Set-Go ELISA kits (eBioscience).

Naive CD4⁺ T cells (CD4⁺CD45RB^{high}CD25⁻) were isolated from total CD4⁺ T cells by FACS sorting. For T-cell differentiation, naive CD4⁺ T cells were cultured in 48-well plates coated with 1 μ g ml⁻¹ of goat anti-hamster antibody (USBiological, Salem, MA) in complete IMDM medium with soluble anti-CD3 antibody (1 μ g ml⁻¹) and anti-CD28 antibody (2 μ g ml⁻¹). For Th1 differentiation, recombinant mouse IL-12 (10 ng ml⁻¹) and neutralizing anti-IL-4 antibody (10 μ g ml⁻¹) were added into the culture. For Th17 differentiation, recombinant mouse IL-6 (20 ng ml⁻¹), recombinant

human TGF- β (4 ng ml⁻¹), anti-IL-4 antibody (10 μ g ml⁻¹), and anti-IFN γ antibody (10 μ g ml⁻¹) were added. For Treg cells differentiation, recombinant human TGF- β (10 ng ml⁻¹), and recombinant mouse IL-2 (100 U ml⁻¹) were added. At day 2, recombinant mouse IL-2 (20 U ml⁻¹) was added into the Th1 culture. After 5 days, cells were collected for re-stimulation and analysis.

Flow cytometry and intracellular staining. Flow cytometry data were acquired in a C6 Accuri flow cytometer (BD Biosciences) and analyzed with FlowJo software (Tree Star, Ashland, OR). For the measurement of intracellular cytokines, CD4⁺ T cells were stimulated with anti-CD3 (5 μ g ml⁻¹) and anti-CD28 (1 μ g ml⁻¹) antibodies in the presence of GolgiStop (BD Biosciences). Cytokines were analyzed using antibodies to IL-17A, IFN- γ , or Foxp3 (all from eBioscience) according to the manufacturer's instructions.

RNA isolation and quantitative reverse transcription-PCR. Reverse transcription-PCR primers for specific target genes were designed based on their reported sequences and synthesized by IDT Technologies (Coralville, IA). RNA isolation and quantitative PCR were carried out as previously described.¹⁰

Evaluation of colitis. Colons of co-housed *Il10*^{-/-} and *Il10*^{-/-}/*Dusp6*^{-/-} mice were analyzed for two parameters; crypt length and inflammatory cell infiltration. The histologic scoring of these parameters was performed as described.¹⁰

Culture of colonic explants. Three to four centimeters colonic samples were weighed and extensively washed in RPMI medium containing 100 μ g ml⁻¹ of streptomycin and 100 U ml⁻¹ of penicillin. Then, the explants were cultured for 24 h in complete RPMI medium at 37 °C and 5% CO₂. Culture supernatants were then collected and cytokine levels measured using Ready-Set-Go ELISA kits (eBioscience).

Proliferation assays. CFSE labeling was used for proliferation assays following a standard protocol. Briefly, a 10 μ M solution of CFSE was prepared in phosphate-buffered saline (PBS)/0.1% bovine serum albumin (BSA). FACS-sorted naive CD4⁺ T cells (CD4⁺CD45RB^{high}CD25⁻) were washed once with PBS and resuspended at 2.5 \times 10⁶ cells ml⁻¹ in pre-warmed PBS/0.1% BSA. While vortexing cells, one volume of CFSE solution was added to one volume of cells for a final concentration of 5 μ M CFSE. Cells were then incubated at room temperature for 10 min without agitation. While vortexing cells, the reaction was quenched with three times the staining volume of ice-cold PBS and the cells were set-aside on ice for 2 min. The cells were then washed twice with 10 ml of complete RPMI, counted and resuspended at 5 \times 10⁵ CD4⁺ cells ml⁻¹. CFSE-labeled cells were then cultured in a round-bottom 96-well plate coated with 1 μ g ml⁻¹ of goat anti-hamster antibody and stimulated with 1 μ g ml⁻¹ of soluble anti-CD3 and 2 μ g ml⁻¹ of anti-CD28 antibodies. After 48 and 72 h, cells were collected and CFSE fluorescence intensity was analyzed by flow cytometry.

Treg suppression assay. The *in vitro* suppression assay protocol was performed in the absence of antigen-presenting cells, with minor modifications of a method previously described.²⁹ Briefly, naive (CD4⁺CD45RB^{high}CD25⁻) and regulatory (CD4⁺CD45RB^{low}CD25⁺) T cells were isolated from a single-cell suspension of splenocytes by immunomagnetic selection and FACS sorting. After sorting, naive T cells were labeled with CFSE as indicated above, counted and adjusted to 5 \times 10⁵ ml⁻¹ in complete RPMI culture media. Unlabeled Tregs were adjusted to 2.5 \times 10⁵ ml⁻¹. Cells were then co-cultured in a round-bottom 96-well plate coated with 1 μ g ml⁻¹ of goat anti-hamster antibody at a Treg:Tnaive cell ratio of 1:2, 1:4, 1:8, and 1:16. Finally, the cells were stimulated with 1 μ g ml⁻¹ of soluble anti-CD3 and 2 μ g ml⁻¹ of anti-CD28 antibodies. After 72 h, the cells were collected and proliferation of naive T cells was analyzed according to CFSE fluorescence by flow cytometry.

In vivo ERK inhibition. Mice were treated with the ERK inhibitor PD0325901, at a dose of 10 mg kg⁻¹ (preventive treatment) or 25 mg kg⁻¹ (curative treatment), following the procedure previously described.²⁸

Immunoblotting. For western blot analysis, CD4⁺ T cells were stimulated and total cell lysates were obtained in lysis buffer containing 0.15 M NaCl, 10 mM HEPES, 0.1 mM EDTA, 0.1 mM EGTA, 1 mM NaF, 1 mM Na₃VO₄, 10 mM KCl, 0.5% NP-40, and protease inhibitor cocktail (10%, vol/vol; Sigma-Aldrich). Proteins (20 µg per lane) were then boiled at 95 °C in the presence of LDS sample buffer and 2-mercaptoethanol (Life Technologies), subjected to SDS-polyacrylamide gel electrophoresis and then transferred to Immobilon-P nitrocellulose membranes (Bio-Rad, Hercules, CA). Membranes were blocked for 30 min in 3% BSA and 0.05% Tween 20 in PBS and incubated overnight with the appropriate primary antibodies, then washed and incubated for 1 h at room temperature with the corresponding anti-mouse or anti-rabbit IgG-HRP secondary antibody (Jackson ImmunoResearch, West Grove, PA). The activity of membrane-bound peroxidase was detected using the ECL system (Thermo Scientific, Waltham, MA).

Statistical analysis. Continuous variables are displayed as mean ± s.d. or mean ± s.e.m., and categorical variables as frequencies or percentages. The Kolmogorov–Smirnov test was used to test normality of continuous variables. Statistical differences between groups were analyzed using the nonparametric Mann–Whitney *U*-test for quantitative data and χ^2 -test for categorical data. Multiple comparisons for quantitative data were assessed by the analysis of variance test followed by the Bonferroni correction. All *P*-values are two-tailed, and *P*-values < 0.05 were considered significant. All calculations were performed using GraphPad Prism 6.0 or SPSS 16.0 software (Chicago, IL).

SUPPLEMENTARY MATERIAL is linked to the online version of the paper at <http://www.nature.com/mi>

ACKNOWLEDGMENTS

We thank Dr J. Molkentin (Cincinnati Children's Hospital Medical Center, Cincinnati, OH) for providing the *Dusp6*^{-/-} mice and Dr Mary P. Corr (Division of Rheumatology, Allergy and Immunology, UC San Diego) for scientific advice. This work was supported by grants CP10/00417 from the Institute of Health Carlos III (Madrid, Spain), Career Development Award #2746 from the Crohn's and Colitis Foundation of America (CCFA), C-05/2012 grant from FISABIO research foundation (Valencia, Spain), and US National Institutes of Health grants AI095623 and DK35108.

DISCLOSURE

The authors declare no conflict of interest.

© 2015 Society for Mucosal Immunology

REFERENCES

- Zassadowski, F., Rochette-Egly, C., Chomienne, C. & Cassinat, B. Regulation of the transcriptional activity of nuclear receptors by the MEK/ERK1/2 pathway. *Cell Signal* **24**, 2369–2377 (2012).
- Keyse, S.M. Protein phosphatases and the regulation of mitogen-activated protein kinase signalling. *Curr. Opin. Cell Biol.* **12**, 186–192 (2000).
- Muda, M. *et al.* The dual specificity phosphatases M3/6 and MKP-3 are highly selective for inactivation of distinct mitogen-activated protein kinases. *J. Biol. Chem.* **271**, 27205–27208 (1996).
- Stewart, A.E., Dowd, S., Keyse, S.M. & McDonald, N.Q. Crystal structure of the MAPK phosphatase Pyst1 catalytic domain and implications for regulated activation. *Nat. Struct. Biol.* **6**, 174–181 (1999).
- Maillet, M., Purcell, N.H., Sargent, M.A., York, A.J., Bueno, O.F. & Molkentin, J.D. DUSP6 (MKP3) null mice show enhanced ERK1/2 phosphorylation at baseline and increased myocyte proliferation in the heart affecting disease susceptibility. *J. Biol. Chem.* **283**, 31246–31255 (2008).
- Bermudez, O., Jouandin, P., Rottier, J., Bourcier, C., Pages, G. & Gimond, C. Post-transcriptional regulation of the DUSP6/MKP-3 phosphatase by MEK/ERK signaling and hypoxia. *J. Cell Physiol.* **226**, 276–284 (2011).
- Owens, D.M. & Keyse, S.M. Differential regulation of MAP kinase signalling by dual-specificity protein phosphatases. *Oncogene* **26**, 3203–3213 (2007).
- Marchetti, S. *et al.* Extracellular signal-regulated kinases phosphorylate mitogen-activated protein kinase phosphatase 3/DUSP6 at serines 159 and 197, two sites critical for its proteasomal degradation. *Mol. Cell Biol.* **25**, 854–864 (2005).
- Bermudez, O., Marchetti, S., Pages, G. & Gimond, C. Post-translational regulation of the ERK phosphatase DUSP6/MKP3 by the mTOR pathway. *Oncogene* **27**, 3685–3691 (2008).
- Gonzalez-Navajas, J.M. *et al.* TLR4 signaling in effector CD4⁺ T cells regulates TCR activation and experimental colitis in mice. *J. Clin. Invest.* **120**, 570–581 (2010).
- Kuhn, R., Lohler, J., Rennick, D., Rajewsky, K. & Muller, W. Interleukin-10-deficient mice develop chronic enterocolitis. *Cell* **75**, 263–274 (1993).
- Roers, A. *et al.* T cell-specific inactivation of the interleukin 10 gene in mice results in enhanced T cell responses but normal innate responses to lipopoly-saccharide or skin irritation. *J. Exp. Med.* **200**, 1289–1297 (2004).
- Kim, S.C. *et al.* Variable phenotypes of enterocolitis in interleukin 10-deficient mice monoassociated with two different commensal bacteria. *Gastroenterology* **128**, 891–906 (2005).
- Madsen, K.L. Inflammatory bowel disease: lessons from the IL-10 gene-deficient mouse. *Clin. Invest. Med.* **24**, 250–257 (2001).
- Li, Q.J. *et al.* miR-181a is an intrinsic modulator of T cell sensitivity and selection. *Cell* **129**, 147–161 (2007).
- Bettini, M.L. & Kersh, G.J. MAP kinase phosphatase activity sets the threshold for thymocyte positive selection. *Proc. Natl Acad. Sci. USA* **104**, 16257–16262 (2007).
- Chang, C.F., D'Souza, W.N., Ch'en, I.L., Pages, G., Pouyssegur, J. & Hedrick, S.M. Polar opposites: Erk direction of CD4 T cell subsets. *J. Immunol.* **189**, 721–731 (2012).
- Luo, X., Zhang, Q., Liu, V., Xia, Z., Pothoven, K.L. & Lee, C. Cutting edge: TGF- β -induced expression of Foxp3 in T cells is mediated through inactivation of ERK. *J. Immunol.* **180**, 2757–2761 (2008).
- Altan-Bonnet, G. & Germain, R.N. Modeling T cell antigen discrimination based on feedback control of digital ERK responses. *PLoS Biol.* **3**, e356 (2005).
- Cao, W. *et al.* Leukemia inhibitory factor inhibits T helper 17 cell differentiation and confers treatment effects of neural progenitor cell therapy in autoimmune disease. *Immunity* **35**, 273–284 (2011).
- Liu, H., Yao, S., Dann, S.M., Qin, H., Elson, C.O. & Cong, Y. ERK differentially regulates Th17- and Treg-cell development and contributes to the pathogenesis of colitis. *Eur. J. Immunol.* **43**, 1716–1726 (2013).
- Tan, A.H. & Lam, K.P. Pharmacologic inhibition of MEK-ERK signaling enhances Th17 differentiation. *J. Immunol.* **184**, 1849–1857 (2010).
- Li, G. *et al.* Decline in miR-181a expression with age impairs T cell receptor sensitivity by increasing DUSP6 activity. *Nat. Med.* **18**, 1518–1524 (2012).
- Tanzola, M.B. & Kersh, G.J. The dual specificity phosphatase transcriptome of the murine thymus. *Mol. Immunol.* **43**, 754–762 (2006).
- Betts, M.R. *et al.* Sensitive and viable identification of antigen-specific CD8⁺ T cells by a flow cytometric assay for degranulation. *J. Immunol. Methods* **281**, 65–78 (2003).
- Betts, M.R. & Koup, R.A. Detection of T-cell degranulation: CD107a and b. *Methods Cell Biol.* **75**, 497–512 (2004).
- Barrett, S.D. *et al.* The discovery of the benzhydroxamate MEK inhibitors CI-1040 and PD 0325901. *Bioorg. Med. Chem. Lett.* **18**, 6501–6504 (2008).
- Lee, S.H. *et al.* ERK activation drives intestinal tumorigenesis in *Apc*^(*trr*/+) mice. *Nat. Med.* **16**, 665–670 (2010).
- Collison, L.W. & Vignali, D.A. *In vitro* Treg suppression assays. *Methods Mol. Biol.* **707**, 21–37 (2011).
- Ivanov, I.I. *et al.* Specific microbiota direct the differentiation of IL-17-producing T-helper cells in the mucosa of the small intestine. *Cell Host Microbe* **4**, 337–349 (2008).

31. Lang, R., Hammer, M. & Mages, J. DUSP meet immunology: dual specificity MAPK phosphatases in control of the inflammatory response. *J. Immunol.* **177**, 7497–7504 (2006).
32. Patterson, K.I., Brummer, T., O'Brien, P.M. & Daly, R.J. Dual-specificity phosphatases: critical regulators with diverse cellular targets. *Biochem. J.* **418**, 475–489 (2009).
33. Liu, Y., Shepherd, E.G. & Nelin, L.D. MAPK phosphatases—regulating the immune response. *Nat. Rev. Immunol.* **7**, 202–212 (2007).
34. Berg, D.J. *et al.* Enterocolitis and colon cancer in interleukin-10-deficient mice are associated with aberrant cytokine production and CD4(+) TH1-like responses. *J. Clin. Invest.* **98**, 1010–1020 (1996).
35. Yen, D. *et al.* IL-23 is essential for T cell-mediated colitis and promotes inflammation via IL-17 and IL-6. *J. Clin. Invest.* **116**, 1310–1316 (2006).
36. Montufar-Solis, D., Schaefer, J., Hicks, M.J. & Klein, J.R. Massive but selective cytokine dysregulation in the colon of IL-10^{-/-} mice revealed by multiplex analysis. *Int. Immunol.* **20**, 141–154 (2008).
37. Kamakura, S., Moriguchi, T. & Nishida, E. Activation of the protein kinase ERK5/BMK1 by receptor tyrosine kinases. Identification and characterization of a signaling pathway to the nucleus. *J. Biol. Chem.* **274**, 26563–26571 (1999).
38. Abraham, S.M. *et al.* Antiinflammatory effects of dexamethasone are partly dependent on induction of dual specificity phosphatase 1. *J. Exp. Med.* **203**, 1883–1889 (2006).
39. Hammer, M. *et al.* Control of dual-specificity phosphatase-1 expression in activated macrophages by IL-10. *Eur. J. Immunol.* **35**, 2991–3001 (2005).
40. Zhao, Q. *et al.* MAP kinase phosphatase 1 controls innate immune responses and suppresses endotoxic shock. *J. Exp. Med.* **203**, 131–140 (2006).